Observation of Wannier-Stark localization by electroreflectance spectroscopy

K. Gibb
Institute for Microstructural Sciences, National Research Council, Ottawa, Canada K1A 0R6

M. M. Dignam
AT&T Bell Laboratories, Murray Hill, New Jersey 07974

J. E. Sipe
Department of Physics, University of Toronto, Ontario, Canada M5S 1A7

A. P. Roth
Institute for Microstructural Sciences, National Research Council, Ottawa, Canada K1A 0R6
(Received 17 December 1992; revised manuscript received 5 May 1993)

Wannier-Stark localization in strained-layer $In_xGa_{1-x}As$-GaAs superlattices is measured using electroreflectance (ER) spectroscopy at 4.5 K. Analysis of the ER data reveals third-derivative line shapes for two samples biased near flat band, which become more first-derivative-like at high applied fields. The exciton transition energies obtained from the line-shape analysis are in good agreement with both photocurrent measurements and exciton Stark ladder calculations for fields greater than 5 kV cm^{-1}. The flat-band ER spectra of the two superlattices reveal distinct features due to their finite sizes, not predicted by the Krönig-Penney model.

INTRODUCTION

Derivative techniques such as photoreflectance[1-4] (PR) and electroreflectance[5,6] (ER) are increasingly being used to characterize quantum-well and superlattice structures, where both techniques provide an increased sensitivity to optical features with respect to the more common photocurrent measurements. Both ER and PR utilize an electric-field-induced perturbation to the samples' dielectric function to generate measurable optical features at critical points in the semiconductor band structure. We present the results of a combined first and third-derivative line-shape analysis of electroreflectance data for two superlattices at successive electric fields ranging from flat band to 25 kV cm^{-1}. The exciton transition energies obtained from this line-shape analysis are found to be in good agreement with photocurrent measurements and exciton Stark ladder calculations.

The electroreflectance line shape for a single transition under low-field conditions is given by

$$\frac{\Delta R}{R}=\mathrm{Re}(e^{i\theta_j}\{E_j-\hbar\omega-i\Gamma_j\}^{-m_j}) , \quad (1)$$

where E_j is the energy of the transition, $\hbar\omega$ is the incident photon energy, Γ_j is the line-shape broadening parameter, and θ_j is a phase factor. The parameter m_j depends upon the critical point type for the transition, and order of derivative used. A first-derivative line shape, $m=1$, is expected for quantum wells, though strong exciton transitions can result in $m=2$. The extended states existing in superlattices under flat-band conditions are expected to result in third-derivative line-shape functions, $m=3$, though indications are that superlattices are best fitted as a mixture of first- and third-derivative line shapes.[1-4] In spite of the reflectivity being a nonlinear function of the dielectric function of the material, a simple summation of the real component of Eq. (1) has yielded good results for the analysis of superlattices.[1-4]

A simple, single-particle, tight-binding model for the Wannier-Stark ladder was presented by Bleuse, Bastard, and Voisin.[7] This model shows the extended states of the superlattice at flat band as gradually localizing with increasing electric field, to become single quantum-well-like (Stark ladder states) at large applied fields. The interband transition energies between the Stark ladder states in the conduction and valence bands at large fields are given by

$$E_p=E_0+pqFd , \quad (2)$$

where E_0 is the isolated quantum-well transition energy, F the electric field, d the superlattice period, and p the Stark ladder index. This equation breaks down at weak fields where the individual Stark ladder states converge to a series of discrete levels at flat band, distributed between the superlattice minizone center (Γ) and edge (Π) points.[8] The high-field Stark ladder result [Eq. (2)] can be improved by the inclusion of the exciton binding energy which may be calculated variationally,[9] yielding values of 8.5 and 4 meV for the $p=0$ and $p=-1$ Stark ladders for our samples. This allows for a comparison between the measured exciton and calculated interband transition energies.

However, the exciton Stark ladder calculations of Whittaker[10] and Dignam and Sipe[11,12] offer considerable improvement. In the latter case, striking success has been achieved in the analysis of the data of Agullo-Rueda *et al.* for an $Al_xGa_{1-x}As$-GaAs superlattice,[11,12] and it is this calculation method that we employ here. Briefly, we

use a tight-binding basis of localized two-well exciton states to form the "exciton Wannier function." The calculation is performed for an infinite superlattice but the maximum electron-hole separation is limited to 51 periods. No appreciable change in the results was found when a larger basis set was used. A smaller basis set will result in changes to the calculated weak-field exciton transition energies, particularly for energies less than the $p=0$ Stark ladder. Hence, the small number of periods (10) in our superlattices is expected to be observed in the weak-field spectra, as discrepancies between the measured and calculated exciton transition energies for the $-p$ Stark ladders.

EXPERIMENTS

Two $In_xGa_{1-x}As$-GaAs strained-layer superlattices were grown by low-pressure metalo-organic vapor-phase epitaxy (MOVPE) on n^+-doped GaAs substrates, and then fabricated into Schottky diode. The induced strain in the $In_xGa_{1-x}As$ layers results in splitting of the light-hole and heavy-hole valence bands so that they may be treated separately in our calculations. The grown layers consist of an undoped GaAs buffer layer, ten-period strained $In_xGa_{1-x}As$-GaAs superlattice, and an undoped GaAs cap layer. Ohmic contacts were alloyed onto the GaAs substrates, while 15-nm semi-transparent gold Schottky contracts were evaporated onto the cap layers. The device structure properties are listed in Table I.

TABLE I. Sample structures.

Sample	H145	L073
In % well	12.8	6.5
Well (nm)	2.5	5.1
Barrier (nm)	9.0	5.0
Buffer (μm)	1.8	0.5
Cap (nm)	10	120

The electroreflectance measurements were performed with the samples maintained at 4.5 K in an exchange-gas cryostat. A conventional electroreflectance apparatus was used except that the static reflectivity R was not recorded, being smoothly varying over the spectral range of our measurements. The ratio $\Delta R/R$ was typically 1×10^{-4} and the modulated electric field was kept near 500 V cm^{-1} peak to peak ensuring a small perturbation to the superlattices.

The material parameters used in the exciton Stark ladder calculations are obtained by interpolation of the material parameters for the two binaries InAs and GaAs.[13] The alloy composition of the wells and layer thicknesses of the superlattices were determined from x-ray measurements, as well as by fitting the near flat-band photocurrent data using a one-band Krönig-Penney model. The in-plane electron and heavy-hole masses differ from the simple linear interpolation due to strain effects. Here we use an in-plane mass of $0.067m_0$ for the electron, and estimate the heavy-hole masses as $0.16m_0$ and $0.19m_0$ for L073 and H145, respectively.[14]

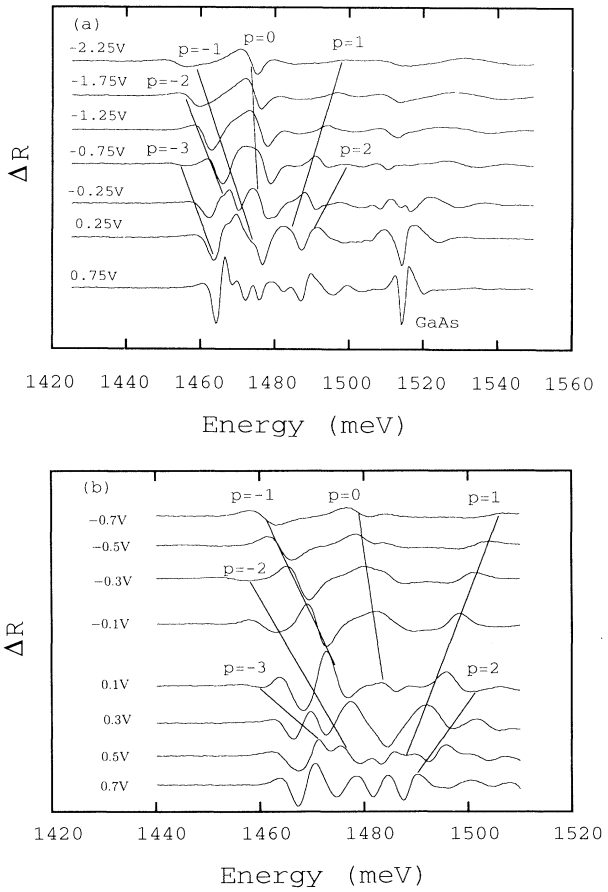

FIG. 1. Bias-dependent electroreflectance spectra for $In_xGa_{1-x}As$-GaAs superlattices. Wannier-Stark ladders are indicated by solid lines. (a) Sample H145, (b) sample L073.

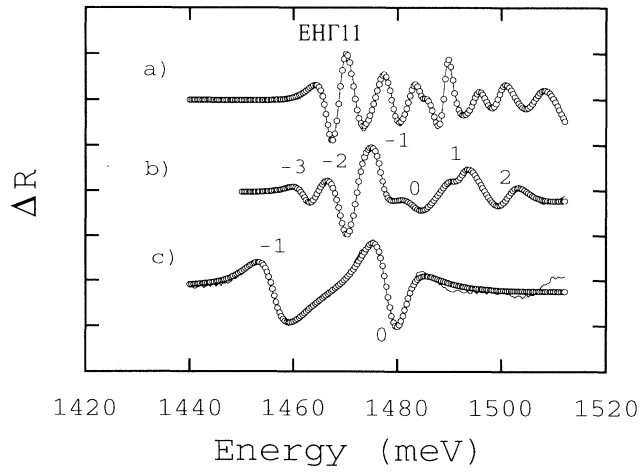

FIG. 2. Measured (solid lines) and calculated ER line-shape (open circles) electroreflectance spectra for L073. Curve *a*, under flat-band conditions $V_{bias}=0.8$ V, fitted using third-derivative line-shape functions. *b*, at 0.2-V bias, using a mixture of first- and third-derivative functions. *c*, at -1-V bias, using predominantly first-derivative functions. Stark ladder transitions are indicated by their indices.

RESULTS

The bias-dependent electroreflectance spectra for H145 and L073 are shown in Figs. 1(a) and 1(b), respectively. In both cases the near flat-band spectra, or lower curves, reveal a number of third-derivative-like line shapes. The flat band is taken to be at 0.8 V. Increasing the reverse bias causes the structures to split away from each other as the Wannier-Stark ladder transitions marked by solid lines. The line shapes appear more first-derivative-like at high applied fields indicating Stark localization.

The near flat-band spectra for the two samples reveal several intense oscillatory structures reminiscent of the expected Γ and Π point interband transitions of the superlattice. The remaining structures are then unexpected. However, the finite size of the superlattices, 10 periods, causes the zero-field eigenstate energies of the 10 wells to form discrete levels. The electron levels associated with the conduction-band superlattice potential for

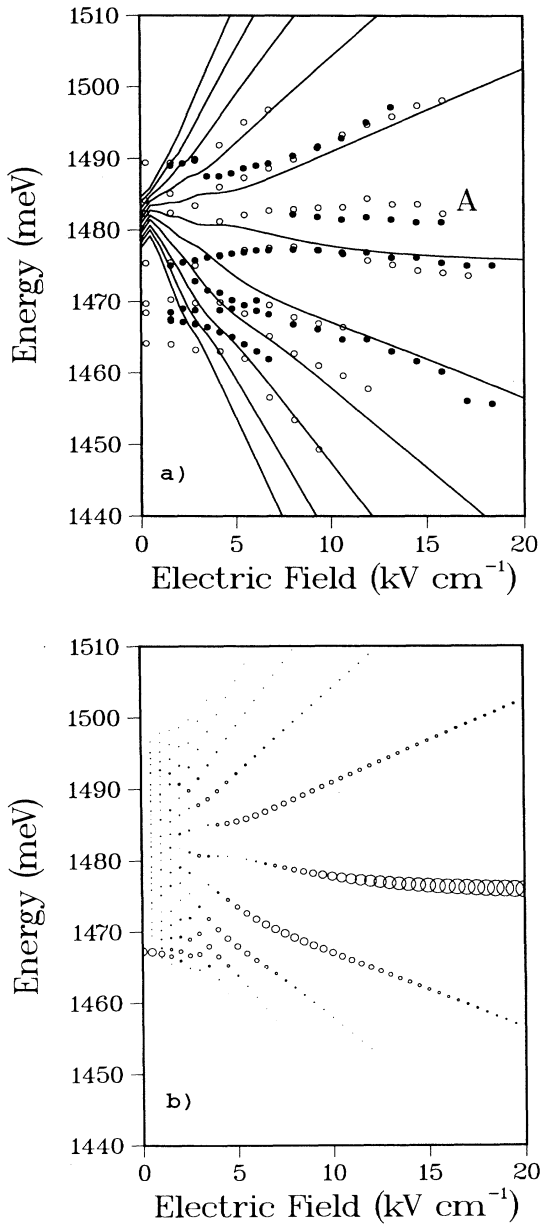

FIG. 3. (a) Field-dependent Stark ladder transition energies for H145, as measured using photocurrent (solid circles), electroreflectance (open circles), and calculated (solid lines) data. Measurements were performed at 4.5 K. The feature labeled *A* is believed to be due to a monolayer thinner well in the superlattice. (b) Calculated oscillator strengths (proportional to circle size) and transition energies for H145.

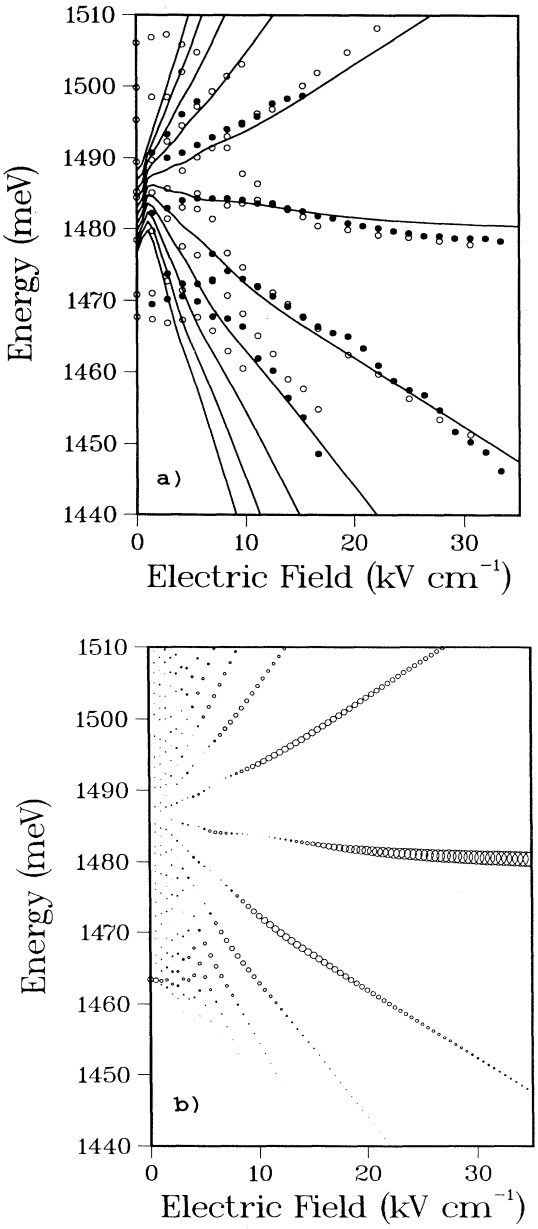

FIG. 4. (a) Electric-field-dependent Stark ladders for L073, from photocurrent (solid circles), electroreflectance (open circles), and calculated (solid lines) data. (b) Calculated oscillator strengths for L073.

both samples are separated by 2–5 meV when the Coulomb interaction is ignored. This is close to the observed spacing between the peaks.

Our line-shape analysis using Eq. (1) allows both first- and third-derivative line-shape functions to be used for each transition. These are coupled by the same transition energy E_j, while the remaining parameters θ_j and Γ_j are left uncoupled. E_j, θ_j, and Γ_j are varied in a least-squares fitting algorithm until a minima is achieved. Up to 18 line-shape functions are used in our fits, with two functions being used per transition. The results of this fitting process for the flat band or 0.8, 0.2, and -1.0 V bias spectra for L073 are shown in Fig. 2, curves *a*, *b*, and *c*, respectively, where the calculated spectra are shown as open symbols, and the experimental data as solid lines. The fitted transition energies are labeled by their Stark ladder indices. The flat-band spectrum (Fig. 2, curve *a*) has been fitted using only the third-derivative line shapes, while the 0.2- and -1.0-V spectra (curves *b* and *c*) have been fitted as mixtures of first and third-derivatives. The magnitude of the first-derivative component in the spectra becomes greater with increasing reverse bias, though the fraction of first- and third-derivative portions is not the same for each Stark ladder transition.

The electric-field-dependent transition energies obtained from the ER and photocurrent (PC) spectra for H145 are plotted in Fig. 3(a) as open and filled circles, respectively. Good agreement is seen between the measured PC, ER data, and the calculated exciton transition energies (solid lines) for applied fields greater than 5 kV cm^{-1}, with the exception of the peak labeled *A*. We are unable to unambiguously identify the origin of this peak, though a monolayer thinner well in the superlattice yields the same transition energy. At fields less than about 5 kV cm^{-1} the measured transition energies no longer follow the calculated data as precisely. In fact, the ER data shows the Stark ladders converging to discrete levels at zero field, whereas the exciton Stark ladder calculations show all of the oscillator strength being transferred to the Γ point of the superlattice miniband, Fig. 3(b). We believe that these discrete levels arise from the finite number of periods (10) used in the two samples.

The calculated oscillator strengths for H145, shown as the diameter of the open circles in Fig. 3(b), for the $p=-1$ Stark ladder tend to be greater than for the $+1$ Stark ladder. This is observed in the ER data shown in Fig. 1(a) where the amplitude of the $p=-1$ ER peak is somewhat larger than the $p=1$ ER peak. The absorption strength asymmetry for these superlattices is partially due to the excitonic and single-particle asymmetry effects.[11] The electron minband width for H145 is 25 meV, less than the conduction-band-confining potential of 95 mV, making this an intermediate-period superlattice where excitonic effects should dominate giving an increased oscillator strength to the negative index ladders. L073 in contrast has a 42-meV electron miniband width, almost as large as the 49-mV confining potential, making this a short-period superlattice. Here the asymmetry is less pronounced, and is due to the overlap of localized wave functions centered on different wells.[11]

The field-dependent transition energies obtained from the ER and PC spectra for L073, Fig. 4(a), also show the formation of Stark localization with good agreement to the calculated Stark ladders, again for fields greater than 5 kV cm^{-1}. In this case, however, 6 meV has been subtracted from the calculated Stark ladder transition energies. This 6 meV can be accounted for by the $\pm 0.5\%$ uncertainty in the indium composition in the wells making up the superlattice. The calculated oscillator strengths, Fig. 4(b), for the $p=1$ Stark ladder are stronger than the $p=-1$ ladder for fields greater than 20 kV cm^{-1}, while the measured ER peaks in Fig. 1(b) show the opposite behavior. The minus-index PC and ER data both show anticrossing behavior similar to the calculated transfer of oscillator strength from the $p=0$ through $p=-3$ Stark ladders as the field is reduced below 10 kV cm^{-1}. The ER data also reveal the finite size of the superlattice as discrete levels at zero field.

The agreement between the calculated and measured exciton transition energies is poorer for the negative-index ladders for both samples as the field is reduced to zero. This is in part due to the choice of line shapes used in the fitting process of the ER data. We find that using a second-derivative line shape can shift the transition energies by several meV, though the first- and third-derivative functions yields results in better agreement with the PC data. In addition, the fine structure of the calculated exciton transition energies and oscillator strengths at weak fields are dependent upon the number of wells used in our calculations. Our calculations are performed for an infinite superlattice and do not consider edge effects which may become important in the small period (10) superlattices studied in this work. Hence a 10-well calculation is expected to yield better agreement between the measured and calculated exciton transition energies.

In conclusion we have demonstrated the ability to extract the Wannier-Stark ladder transition energies using electroreflectance spectroscopy at liquid-helium temperature. We find that the ER structures are best modeled as a mixture of first- and third-derivative line shapes, though second-derivative line-shape functions will provide a fit but with slightly different transition energies. The determined energies are found to be in good agreement with results from PC data and exciton Stark ladder calculations over a large range of applied fields. The ER data reveals features due to the finite size of the superlattice at very weak fields which were not observed in our PC data, due to the increased sensitivity of ER.

[1]F. H. Pollak and O. J. Glembocki, in *Spectroscopic Characterization Techniques for Semiconductor Technology III*, SPIE Conference Proceedings No. 946, edited by O. J. Glembocki, F. H. Pollak, and F. Ponce (International Society for Optical Engineering, Bellingham, WA, 1988), p. 2.

[2]F. H. Pollak and H. Shen, Superlatt. Microstruct. **6**, 203 (1989).

[3]Y. S. Tang, Semicond. Sci. Technol. **4**, 871 (1989).

[4]Y. S. Tang, J. Appl. Phys. **69**, 8298 (1991).

[5]I. J. Fritz, T. M. Brennan, and D. S. Ginley, Solid State Commun. **75**, 289 (1990).

[6]M. Nakayama, I. Tanaka, T. Doguchi, H. Nishimura, K. Kawashima, and K. Fujiwara, Solid State Commun. **77**, 303 (1991).
[7]J. Bleuse, G. Bastard, and P. Voisin, Phys. Rev. Lett. **60**, 220 (1988).
[8]P. W. A. McIlroy, J. Appl. Phys. **59**, 3532 (1986).
[9]K. Gibb, E. Fortin, and A. P. Roth, Semicond. Sci. Technol. (to be published).
[10]D. M. Whittaker, Superlatt. Microstruct. **7**, 375 (1990).
[11]M. M. Dignam and J. E. Sipe, Phys. Rev. Lett. **64**, 1797 (1990).
[12]M. M. Dignam and J. E. Sipe, Phys. Rev. B **43**, 4097 (1991).
[13]*Numerical Data and Functional Relationships in Science and Technology,* edited by O. Madelung, Landolt-Börnstein, New Series, Group III, Vol. 22 (Springer-Verlag, Berlin, 1988).
[14]R. People and S. K. Sputz, Phys. Rev. B **41**, 8431 (1990).